

(TOPICAL REPORT)

**INTEGRATED RESEARCH FOR PREDICTING HIGHER
DIMENSIONAL PHASE DIAGRAMS WITH EMPHASIS ON
TERNARY DIAGRAMS OF MOLYBDENUM, SILICON, AND
BORON**

[4000013127]

Ning Ma¹, Bernald R. Cooper¹ and Bruce S. Kang²

¹Physics Department

²Mechanical and Aerospace Engineering Department
West Virginia University
Morgantown, WV 26505

SUMMARY

In this report, we present the status of our computational modeling study of ternary system of Molybdenum, Silicon and Boron over a wide range of temperature. We have used Monte Carlo simulation technique to predict the mechanical and thermal properties of these materials. The required total energy of the sample is computed by using a tight-binding (TB) method that allows us to significantly increase the size of the computational data base without reducing the accuracy of the calculations. The Slater-Koster hopping parameters are directly computed from results of full-potential linear muffin-tin orbital (FP-LMTO) calculations through a modified McMahan and Klepeis's approach[1, 2]. The site energies, crystal-field corrections and repulsive potential are fitted in various physical models. The combination

of the methods mentioned above creates an effective approach to the computation of the physical properties of the transition-metal compounds and it can be extended to alloys with more than two components. At present, we have obtained excellent agreement with experiment for Mo and Mo Silicides, especially Mo_3Si . The third component of the ternary system, Boron, is currently under our current investigation.

1 Introduction

Founded by the classic work of Slater and Koster half a century ago[3], the tight-binding method (TB) has experienced a renewed popularity in recent literatures. Although the early TB methods were introduced mainly as an interpolation scheme, their modern decedents have been used to compute electronic structures to achieve roughly the same order of accuracy as the more sophisticated self-consistent first-principles electronic methods. The success of TB is not only due to its apparent advantage of theoretical simplicity and numerical efficiency, but also because it is a method that uses the direct real-space (as opposed to k-space) approach, and thus it has a wide range of applications in problems that lack perfect crystalline symmetries (e.g., defects, impurities, surfaces and interfaces).

Despite the overwhelming success in modeling of single elements[4], recent progress of TB method has not yield fruitful results on intermetallic alloy compounds. Papaconstantopoulos *et.al.* has tabulated TB parameters for a few alloy systems[5], however, we have not heard any success in using these parameters in molecular dynamics or Monte Carlo simulations at the time being. The scarece of TB parameters for compound materials is due to the following difficulties: First, the traditional means to obtain parameters is to fit the TB energy bands to those obtained either from first principles theoretic calculations or from the experiments. The numerical fitting procedure, which performs the standard nonlinear minimization on the merit function, works well only when the number of independent parameters is relatively small. But a typical binary compound material requires over 300 independent parameters. To fit so many parameters simultaneously is prohibitively tedious, and the merit function can easily be trapped into local minimums, resulting in unphysical TB parameters that produce TB bands bearing little resemblance to the original ones. In addition, for simulations of thermodynamic properties (such as entropy, free energy and chemical potentials)

of different solids and liquids, it is highly demanding that the parameters be transferable. However, parameters obtained through fitting lack physical meanings, therefore, their validity are usually limited to the same crystal structure as they are originally fitted for.

In this report, we present an implementation of TB method that overcomes most of the difficulties described in the above. In this scheme, we followed the method of McMahan and Klepeis[1, 2] to extract all hopping TB parameters *directly* from the Hamiltonian and overlap matrices computed by first-principles full-potential linear muffin-tin orbital (FP-LMTO) method[6, 7], avoiding the difficulties of fitting procedure. Additional calibration of energy is performed to improve the transferability of the parameters. The idea of obtaining TB parameters directly from first-principles calculation dates back to Andersen *et. al.*[8], and has been continued by other groups[9]. The first serious application of this method on intermetallic materials was done by Djajaputra[7] for Ni Aluminides. Our work can be viewed as an extension to his work in further extracting two-center SK parameters, as well as incorporating other energy parameters, such as on-site and repulsive potential, to form a representation for the total energy and subsequently using them in Monte Carlo (MC) simulation. Our on-site parameters were obtained through numerical fittings, which is quite different from McMahan's original scheme. We feel this way preserves the physical meanings of these parameters, making them easier to transfer to other structures. Since the fitting is done for one angular momentum at a time, there is not too much of numerical burden. Finally, we augmented the TB band energy with an additional repulsive potential part. We used an embedded atom method (EAM) scheme and superposition of contracted atomic density approximation to facilitate the fitting of repulsive energy parameters.

We choose the ternary system of Mo, Si and B as our example materials, because they are currently being developed for high temperature ($> 1000^{\circ}\text{C}$) structural applications[10]. In the processing of these materials, it is critical to be able to predict phase development under varying thermodynamic conditions, with variations in composition. The technique we mentioned above will allow us to treat a unit cell of very large size, i.e., with a very large number of independently behaving atoms. This will allow us conveniently and accurately to predict effects of variation in stoichiometry and of additives. In the present report we first deal with modeling of Mo and Si, with special interest in the modeling of Mo_3Si (cubic A15, see Fig.1). The parameters used in Mo_3Si are demonstrated to be transferable to other Mo Silicides. The

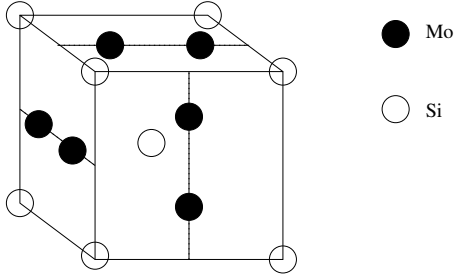


Figure 1: The cubic A15 structure for Mo_3Si : The Mo atoms (black circles) form lines bi-secting the cubic surfaces, and Si atoms (white circles) occupy the bcc lattice.

inclusion of the third component, Boron, are left for our future work.

In the following sections, we shall first present a detailed description of the method in Sec.2, then the tests of accuracy and transferability in Sec.3, followed by Monte Carlo simulation results in Sec.4, and the future plan in Sec.5.

2 Methodology

As usual, we separate the total energy into TB band energy part and a short range repulsive potential part.

$$E_{\text{tot}} = E_{\text{band}} + E_{\text{rep}}. \quad (1)$$

The above separation of total energy involves some arbitrariness. In some TB total energy schemes (notably Papaconstantopoulos *et.al.*[13]), the repulsive potential is entirely absorbed by the band energy as a chemical potential shift. While this treatment simplifies the problem by reducing the number of parameters to be fitted, it ultimately obscures the physical meaning of TB parameters. For example, the TB energy is no longer purely attractive in this model, and the parameters will have to be able to represent both short range repulsion and long range attraction. Considering these shortcomings, we shall keep both terms in our formulation. The arbitrariness of the energy separation will be partially remedied later in the procedure of calibration of the band energy.

2.1 The Band Energy

In the so called non-orthogonal TB model, one computes the Hamiltonian and overlap matrices H and S , and solves the generalized eigen problem:

$$(H - \varepsilon_i S)\psi_i = 0. \quad (2)$$

The band energy is obtained by summing the energy eigenvalues up to the chemical potential weighted by Fermi function

$$E_{\text{band}} = \sum_{\varepsilon_i < \varepsilon_F} \varepsilon_i f(\varepsilon_i). \quad (3)$$

Slater and Koster used the two center approximation to express the Hamiltonian and overlap matrix elements as linear combination of a set of parameters known as SK parameters[3]. For example, a hopping ($R \neq 0$) Hamiltonian matrix element may be written as (here we used the McMahan's convention[1])

$$\langle 0lm|H|\mathbf{R}l'm'\rangle = \sum_{\mu} g_{\mu}(lm, l'm', \hat{\mathbf{R}})t_{W\mu}(R), \quad (4)$$

where g_{μ} s are the linear coefficients that depend on the geometric alignment of the involving atomic orbitals, and $t_{W\mu}$ s are the SK parameters that depend only on interatomic distance R .

The inverse problem, namely to determine SK parameters out from given Hamiltonian and overlap matrices, has been considered by McMahan and Klepeis[1, 2]. They found an orthogonality relations among the g_{μ} s to invert Eq.(4):

$$t_{W\mu}(R) = (2 - \delta_{\mu\sigma})^{-1} \sum_{m,m'} g_{\mu}(lm, l'm', \hat{\mathbf{R}})\langle 0lm|H|\mathbf{R}l'm'\rangle. \quad (5)$$

Thus, the procedure of obtaining SK hopping parameters is made straightforward: We first computed the k-space Hamiltonian and overlap matrices for the material using our accurate FP-LMTO[6] method. The matrices were then anti-Fourier transformed into the real space. The above steps have been nicely discribed in detail by Djajaputra[7]. Following Eq.(5), the hopping TB parameters for this particular structure are then obtained.

The above procedure differs from traditional fitting efforts in that all parameters for this structure is *uniquely* determined. It is emphasized in

the original paper that the set of parameters so obtained may not be the most accurate parameters, but is the best possible within the two center approximation, therefore, good transferability is hinted. For intermetallic compounds such as the one we are interested in, the number of parameters is too large to be fitted simultaneously via traditional means. Therefore, this procedure is preferable in its efficiency. In addition, since we are interested in an overall accurate total energy, we can sacrifice the accuracy of individual terms for better transferability.

The hopping parameters $t(R)$ obtained at one volume have values at discrete set of R points corresponding to the interatomic distances for that specific structure. More values at additional R points may be obtained by varying the volume in the FP-LMTO calculation. Note, however, that the SK TB parametrization assumes that the underlying basis orbitals remain fixed as the lattice volume or structure is changed. This is not always possible since by nature the FP-LMTO calculation finds the optimal set of orbitals that minimize the density functional. In the original paper of McMahan *et. al.*[1], a unitary rotation was performed on both Hamiltonian and overlap matrices to ensure a perfectly transferable overlap. Issues of non-transferability was relegated to the Hamiltonian. In our practice, however, we found that if the volume is not varied too much (by less than $\pm 17\%$) and if we restrict the muffin-tin radius to be fixed at all volume calculations, the same overlap functions $s(R)$ share a pretty much the same shape (see Fig.2). Therefore, no unitary rotation is needed. This is partly because we have used only one-kappa for each orbital considered, and that most characteristic information of the orbitals is contained in the muffin-tin region, which is fixed in size. The changing interstitial area, being a small fraction of the total volume, often sees smooth density and potential and becomes less important in affecting the Hamiltonian and overlap matrices. It should be noted that in a typical FP-LMTO calculation, the muffin-tin radius is a variational parameter and should be varied to find the minimum energy. Here, we emphasize on the transferability of the parameters; we leave any deviation from the accurate band energy to be absorbed by the repulsive potential.

Unlike the case of overlap functions, noticeable differences exist among the same Hamiltonian parameters $t(R)$ obtained at different volumes (see Fig.3). It seems that the Hamiltonian parameters depend on the shell number as well as distance. Similar phenomenon can be seen in the $dd\sigma$ plot in Ref.1, as well as being reported in other TB implementations[14], where the scheme of environment-dependent TB parameters that accounts for the

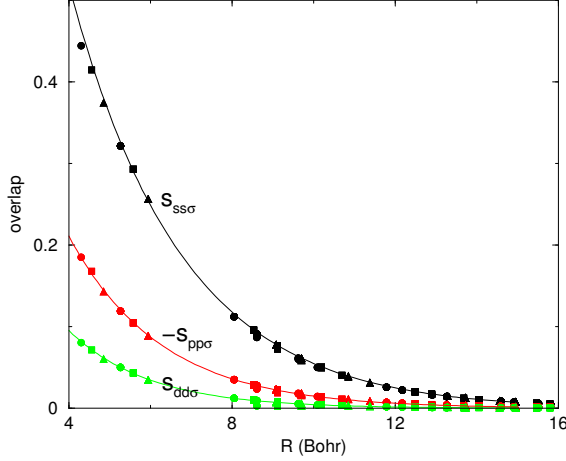


Figure 2: The same overlap hopping parameters $s(R)$ obtained at different volumes.

shell dependence was elaborated. In our case, we found that the problem is caused by the arbitrariness involved in the separation of total energy into valence eigenvalue sum and remaining part in our FP-LMTO formulation. Therefore, it is very important to calibrate the energy reference point for the Hamiltonians before comparing them at different volumes. We chose the energy reference to be the energy level for the inner most core electron (such as e_{1s}) because it is most unlikely to be affected by the bonding environment. After calibration $t(R) \rightarrow t(R) - e_{1s}s(R)$, the new Hamiltonian parameters are plotted in Fig.3, where the improvement over Fig.2 is prominent.

We fit the overlap and calibrated Hamiltonian parameters into the following simple functional form:

$$t(R) = (a_0 + a_1 R)e^{-a_2 R}. \quad (6)$$

Results are tabulated in Table 1. The rms percentage scatter about them is 5% or less considering 15 points at $R < 10$ Bohr (1Bohr=0.529Å). Compared to the scatter of 20% and 32% for $t_{ld\sigma}$ and $t_{dd\sigma}$ reported in Ref.1, our (slightly altered) procedure gives a significant improvement of transferability.

We now turn to the on-site ($R = 0$) parameters. In contrast to the case of hopping parameters, Hamiltonian matrix of a single structure is not adequate to determine all crystal-field parameters except for their certain fixed sums. Ref.1 studied these sums as effective site energies and effective crystal-fields.

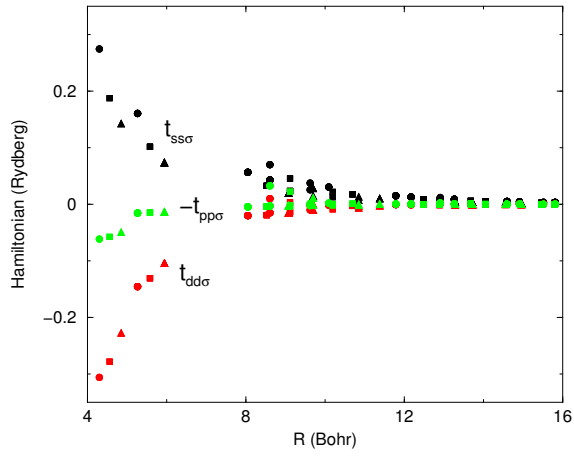


Figure 3: The same Hamiltonian hopping parameters $s(R)$ obtained at different volumes, before energy calibration.

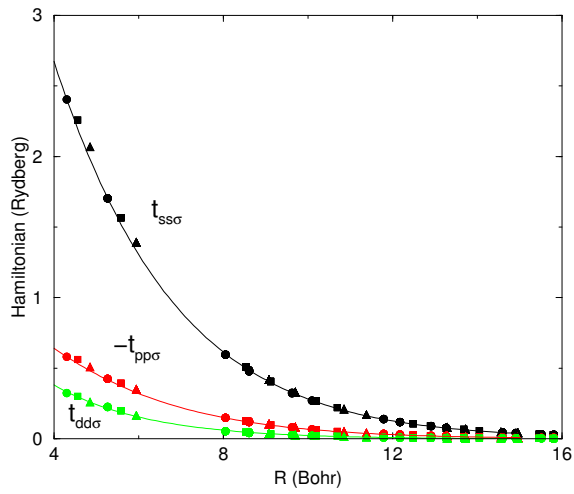


Figure 4: The same Hamiltonian hopping parameters $s(R)$ obtained at different volumes, after energy calibration.

Table 1: σ SK hopping parameters obtained for Mo_3Si . (π and δ SK parameters are available upon request.) All energies are in Rydberg (1Ryd.=13.6eV) and all lengths are in Bohr (1Bohr=0.529Å).

	type	a_0	a_1	a_2		type	a_0	a_1	a_2
$t_{ss\sigma}$	Mo-Mo	9.132	1.972	0.463	$s_{ss\sigma}$	Mo-Mo	2.191	-0.092	0.314
$t_{sp\sigma}$	Mo-Mo	-5.540	0.230	0.315	$s_{sp\sigma}$	Mo-Mo	-1.370	0.053	0.338
$t_{sd\sigma}$	Mo-Mo	3.205	-0.145	0.318	$s_{sd\sigma}$	Mo-Mo	0.595	-0.029	0.304
$t_{ss\sigma}$	Mo-Si	5.871	2.738	0.483	$s_{ss\sigma}$	Mo-Si	2.272	-0.081	0.336
$t_{sp\sigma}$	Mo-Si	-9.233	0.390	0.309	$s_{sp\sigma}$	Mo-Si	-1.821	0.075	0.314
$t_{sd\sigma}$	Mo-Si	5.705	-0.226	0.338	$s_{sd\sigma}$	Mo-Si	0.978	-0.044	0.318
$t_{pp\sigma}$	Mo-Mo	-1.546	-0.747	0.489	$s_{pp\sigma}$	Mo-Mo	-1.233	0.000	0.441
$t_{pd\sigma}$	Mo-Mo	2.158	-0.093	0.348	$s_{pd\sigma}$	Mo-Mo	0.969	-0.000	0.484
$t_{ps\sigma}$	Mo-Si	5.175	-0.214	0.315	$s_{ps\sigma}$	Mo-Si	1.487	-0.028	0.381
$t_{pp\sigma}$	Mo-Si	-4.607	0.197	0.309	$s_{pp\sigma}$	Mo-Si	-1.484	0.022	0.394
$t_{pd\sigma}$	Mo-Si	4.195	-0.087	0.401	$s_{pd\sigma}$	Mo-Si	1.392	0.000	0.470
$t_{dd\sigma}$	Mo-Mo	2.219	-0.114	0.383	$s_{dd\sigma}$	Mo-Mo	0.726	-0.000	0.508
$t_{ds\sigma}$	Mo-Si	3.092	-0.129	0.329	$s_{ds\sigma}$	Mo-Si	0.721	-0.028	0.349
$t_{dp\sigma}$	Mo-Si	-1.476	-0.964	0.515	$s_{dp\sigma}$	Mo-Si	-0.704	0.031	0.340
$t_{dd\sigma}$	Mo-Si	5.182	-0.000	0.495	$s_{dd\sigma}$	Mo-Si	0.942	-0.033	0.440
$t_{ss\sigma}$	Si-Si	10.750	-0.341	0.340	$s_{ss\sigma}$	Si-Si	2.521	-0.000	0.397
$t_{sp\sigma}$	Si-Si	-6.612	-1.429	0.454	$s_{sp\sigma}$	Si-Si	-2.338	0.000	0.400
$t_{sd\sigma}$	Si-Si	5.586	-0.158	0.362	$s_{sd\sigma}$	Si-Si	1.510	-0.000	0.430
$t_{pp\sigma}$	Si-Si	-8.580	0.294	0.331	$s_{pp\sigma}$	Si-Si	-2.209	-0.000	0.404
$t_{pd\sigma}$	Si-Si	6.163	-0.116	0.387	$s_{pd\sigma}$	Si-Si	1.697	-0.000	0.446
$t_{dd\sigma}$	Si-Si	6.198	-0.000	0.462	$s_{dd\sigma}$	Si-Si	1.839	-0.000	0.507

These effective parameters are still directly computable thus possessing the virtue of being free from numerical fitting. However, being pure mathematical convenience, they lack the physical interpretation, therefore are structure and volume dependent, i.e., non-transferable. For our purpose, we use alternative way of numerical fitting to find transferable on-site parameters.

To facilitate the fitting, we made a simplifying assumption that the crystal-fields are just a bunch of delta functions situated at neighboring atomic sites. This is equivalent to applying the averaged potentials of a neighboring site to the smooth tails of the orbitals from the host site. Under this assumption, the integration of potential acting on the wavefunctions can be easily carried out, and the on-site matrix element now becomes:

$$e_{lm} = e_l^0 + \sum_{\mathbf{R} \neq 0} h |\psi_{lm}(\mathbf{R})|^2, \quad (7)$$

where, the summation is over all neighboring atomic sites; e_l^0 is the on-site energy, and h is the coefficient of the delta function or the averaged potential. Both are to be fitted to the diagonal Hamiltonian matrix elements (in real space). In addition, we parametrized the asymptotic behavior of the wavefunction squares in the following form so that orbitals differ only in magnetic number share a common radial part:

$$|\psi_{l,m}(\mathbf{R})|^2 = (b_0 + b_1 R) e^{-b_2 R} |Y_m^l(\hat{\mathbf{R}})|^2. \quad (8)$$

These assumptions enable us to significantly reduce the number of parameters that are needed in fitting while still retaining the physics of the directionality of covalent bonds. The fitting can be done one at a time for each angular momentum, and the results are tabulated in Table2. Note that parameter h appearing in Eq.(7) is absorbed into the bs .

A few remarks are in order: First, in practice we used the set of real combinations of Y_m^l s that have the cubic symmetry. The two groups of Mo d -orbitals resulting from cubic crystal field splitting are fitted individually as though they possess different angular momenta. For Si, such treatment is found to be unnecessary. Second, it should be noted that the calibration of energy reference point mentioned earlier is of equal importance here. To see this, we point out that according to Eq.(7), the volume dependence of e_{lm} should become flat when volume (or interatomic distance) is large. However, without calibration, there is an additional dependence of e_{lm} on the volume due to the shifting energy reference, which does not vanish at large

Table 2: SK on-site parameters obtained for Mo₃Si. All energies are in Rydberg (1Ryd.=13.6eV) and all lengths are in Bohr.

l	type	e_l^0	b_0	b_1	b_2
s	Mo	6.270	2.729	-0.926	0.802
p	Mo	3.649	-2.563	0.000	0.808
d_{yz}	Mo	6.016	-37.999	4.664	0.745
$d_{x^2-y^2}$	Mo	6.080	-24.359	0.000	0.927
s	Si	5.693	0.761	-0.340	0.675
p	Si	6.117	-3.362	0.320	0.523
d	Si	7.305	-2.463	0.000	0.370

volume, thus making fitting to the form Eq.(7) difficult. Finally, comparing the exponential factor a_2 in Table1 and the corresponding b_2 in Table2, we see approximately $b_2 \approx 2a_2$, which hints that our fitted results for the orbital tail square is consistent with the directly computed overlap SK parameters, partially justify our simplifying assumptions.

2.2 The Repulsive Potential

The band energy accounts for the electronic interactions and is purely attractive. To explain the bonding behavior, we need a repulsive potential that includes the ion-ion repulsion and a correction for overcounting of the electron-electron interaction. In addition, we have sacrificed some accuracy for transferability in the modeling of band energy. The inclusion of the repulsive potential will remedy this deficiency.

We implemented the repulsive potential using an EAM scheme, where the repulsive energy is a sum of embedding energies that depend on the local electron densities at all atomic sites:

$$E_{\text{rep}} = \sum_{\mathbf{R}} f(\rho(\mathbf{R})). \quad (9)$$

The functional form of the embedding function f is unknown, and is to be determined by fitting. The electron density at site \mathbf{R} is assumed to be a linear superposition of contracted atomic densities originated from all other sites:

$$\rho(\mathbf{R}) = \sum_{\mathbf{R}' \neq \mathbf{R}} \rho^0(\alpha|\mathbf{R}' - \mathbf{R}|). \quad (10)$$

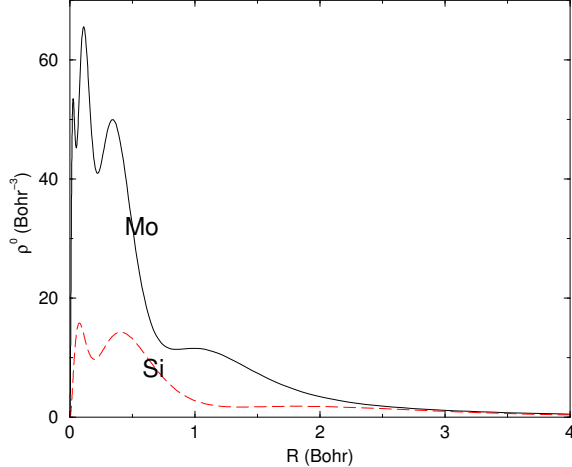


Figure 5: Spherically averaged electron density for Mo (solid line) and Si (dashed line).

In Eq.(10) the atomic density ρ^0 can be obtained accurately by applying first principles methods on an isolated atom. Fig.5 shows the spherically averaged electron density for Mo and Si. The linear superposition of atomic densities may deviate from the real density, however, due to the variational nature of the density functional theory, the change of energy is of second order for a first order change of density. α is a scaling factor for distance which is set to be 1.2 in our calculation. The use of contracted density is motivated by the fact that in the crystal environment the atomic density is distorted by nearby atoms via electronic screening. It also reflects the requirement that the repulsion should be shorter ranged than the attraction for a stable bonding.

Once $\rho(\mathbf{R})$ are computed, we fitted the embedding function f in Eq.(10) to a fourth order polynomial:

$$f(x) = c_0 + c_1x + c_2x^2 + c_3x^3 + c_4x^4. \quad (11)$$

The left hand side of Eq.(10) is taken to be the difference between the total energy obtained with FP-LMTO (using four-kappa linked basis for each angular momentum) and TB band energy computed using our SK parameters obtained earlier, calculated at various volumes. In the FP-LMTO calculation, the 4p semicore electrons of Mo are treated as valence electrons in a separate energy window (to be distinguished from 5p electrons).

3 Tests of Parameters

In this section, we test our parameters for their accuracy and transferability.

3.1 Accuracy Tests

Since our main interest is to use these parameters in MC simulation, we emphasize on the accuracy of overall total energy, not the individual contributing parts. The testing procedure is to see how well our TB total energy scheme can reproduce the results from accurate FP-LMTO calculations. For this purpose, we used distorted structures that are not limited to the original database when parameters are fitted or extracted. (Our original database only consists of uniform expansion or contraction of the volume). The distortions we considered fall into the following two categories.

The elastic distortions are those to obtain mechanic elastic constants. They are intimately related to the acoustic excitations of the crystal. For cubic structure, there are three independent elastic modula: c_{11} , c_{12} and c_{44} , corresponding roughly to longitudinal, transverse and sheer modes. The following three types of distortions are designed to extract these modula[15]: Type I: expanding in x and y direction by γ while compressing in z direction by $(1 + \gamma)^{-2} - 1$, so that the volume is conserved; Type II: expanding all directions by γ , i.e., the uniform expansion; Type III: changing the angle between x and y axis by γ , and expanding in z direction by an amount that conserves the volume. Fig.6 shows the comparison of our TB total energy results and FP-LMTO results under these types of distortions.

The other class of distortions, which is more related to optical vibration modes of the lattice, is to arbitrarily displace atoms out of their equilibrium positions. To retain symmetry so as to facilitate FP-LMTO calculation, we chose the following displacement: moving the nearest neighbor pair of Mo atoms towards or apart by γ . This test is currently in progress.

3.2 Transferability Tests

The transferability, that parameters prepared for one structure or stoichiometry are applicable to a other structures and stoichiometries, is an essential property that is desirable for MC as well as other applications.

The transferability of the hopping SK parameters for Mo_3Si over a range of volumes and distortions for the cubic A15 structure has been discussed

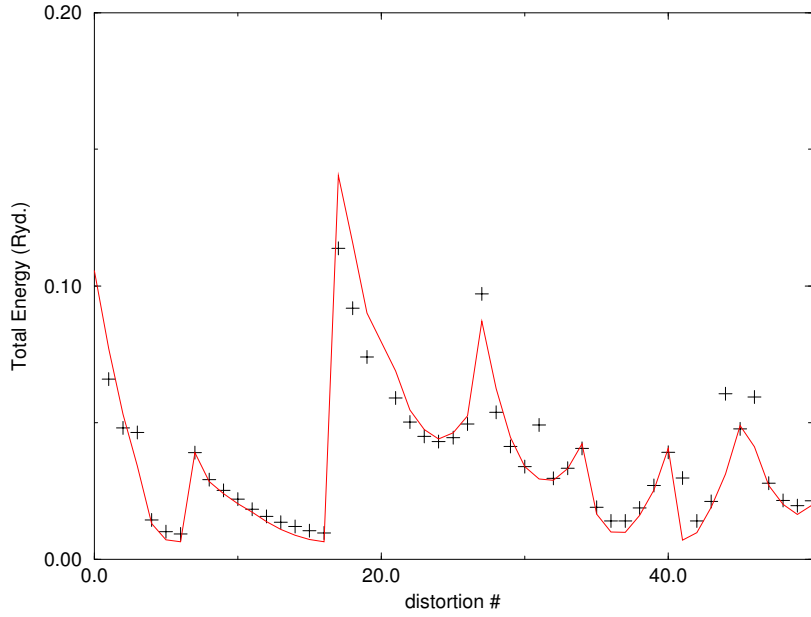


Figure 6: The comparison of FP-LMTO results (plus signs) and TB total energy results (solid line) under elastic distortions. (The figure actually shows only type I and II distortion tests. The type III test is currently in progress. We expect to have updated figure soon.

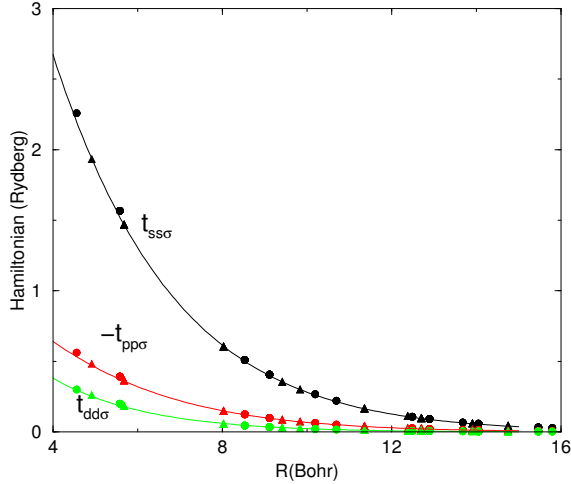


Figure 7: The comparison of two sets of parameters for Mo-Mo. The squares are obtained for A15 Mo_3Si , and the triangles are obtained for bcc Mo.

in the accuracy tests. Here we focus on transferability over the variation of structure and stoichiometry. For this purpose, we independently developed another set of parameters for Mo in α -Mo (bcc.). In preparing the second set, we have carefully set parameters such as muffin-tin radius to be the same value as the first set. The calibration is done in a similar way to make the two sets comparable. The results are plotted in Fig.7. The agreement of the two sets is excellent, indicating very good transferability for our Mo parameters.

The same transferability test for Si in Mo_3Si and cubic diamond Si does not yield the same excellent agreement. See Fig.8. Even for overlap parameters, the discrepancy goes up to about 40% (for $t_{dd\sigma}$). We note that the nearest Si-Si distance is about 4.2\AA in Mo_3Si , but is only about 2.3\AA in diamond cubic Si; the change is about 46%. In contrast, the nearest Mo-Mo distance is 4.6\AA in Mo_3Si and 4.2\AA in α -Mo, only about 10% change. We thus conclude that good transferability is limited to change in nearest neighbor distance not more than 10%.

The transferability of on-site and EAM parameters are currently under our investigation.

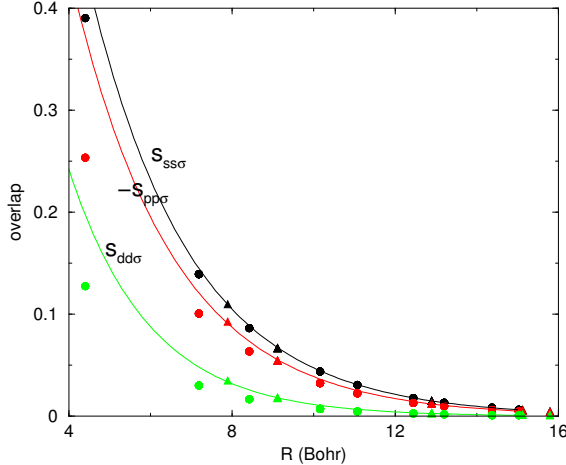


Figure 8: The comparison of two sets of parameters for Si. The squares are obtained for A15 Mo_3Si , and the triangles are obtained for cubic diamond Si.

4 Monte Carlo Simulation

Our accuracy and transferability tests build up our confidence in using these parameters in MC simulation. As an example, we test to predict CTEs for Mo_3Si at various temperatures and compare them with experiment. Calculating CTEs using MC simulation presents a numerical challenge, because the energy is near its minimum when lattice constants are sampled. This implies that the lattice constant can fluctuate wildly without suffer of too much energy penalty. Therefore, more data needs to be sampled before result is converging.

The system simulated consists of 216 atoms ($3 \times 3 \times 3$ supercells). For each MC step, we either randomly displace an randomly chozen atom or change the lattice constant. The chance of these two operations are half and half. We started 13 systems at temperatures ranging from 1200K through 2000K, incremented by 100K, from the same initial configuration of perfect crystal structure. Lattice constants were sampled at every 20 MC steps after the system achieved thermal equilibrium (around 10,000 MC steps). 500 samples were then averaged and their temperature dependence was plotted in Fig.9. We see that for the specified temperature range, the material displays a fairly good linear thermal expansion. The CTEs can be easily read off from the

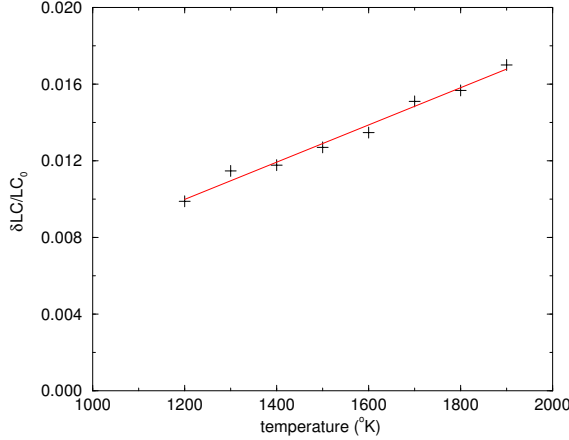


Figure 9: The averaged lattice constants at 13 temperature points. Data obtained from MC simulation

figure.

To relate our theoretical work with experimental results, we have also simulated Mo_{53}Si system using the same set of parameters. Fig.10 shows the sampled average lattice constants at 8 different temperature points. The data were compared with the TMA experimental results, which is conducted on a Mo_{39}Si system. Both results have been offset for comparison, and the agreement is impressive. Since the parameters used in this calculation were originally prepared for Mo_3Si , it is another demonstration of good transferability. Note that the experiment curve has a few sharp peaks at temperature around 900-1300°K. The ‘abnormal’ behavior within this temperature range is believed to be associated with a phase transition, which is manifested in Fig.11, where DTA data shows a transition between an energy-absorbing state and an energy releasing state.

5 Future Work

We modified McMahan’s scheme of obtaining TB parameters directly from FP-LMTO calculations, and developed a set of TB parameters for Mo Silicides systems. Our parameters are accurate enough to compute various static properties such as elastic constants, and reasonably transferable if the near neighbor distance is varied by not more than 10%. We used these parameters

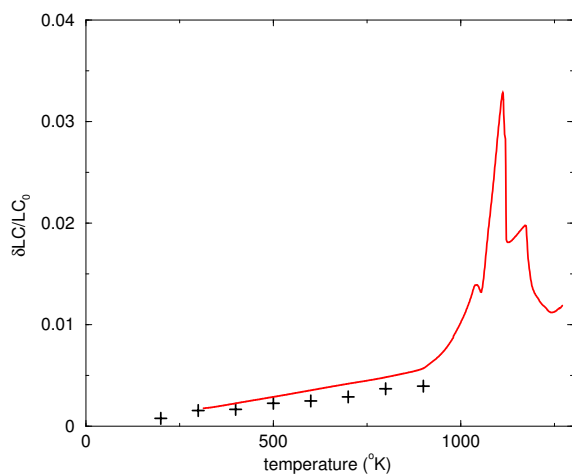


Figure 10: Pluses: lattice constants of Mo_{53}Si obtained by MC; solid curve: (rescaled) linear sizes of Mo_{39}Si obtained by experiment.

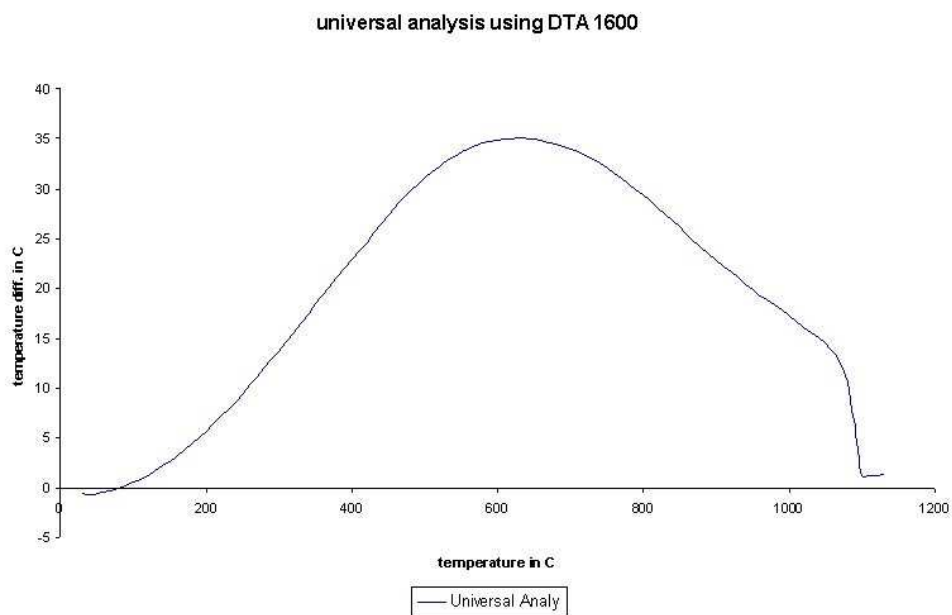


Figure 11: DTA data for the same material.

in MC simulation to compute the CTEs of Mo_3Si and Mo_{53}Si . The result of the latter material is in good agreement with our experiment findings. To our knowledge, this work is the first TB molecular dynamics or MC modeling of intermetallic compound materials.

Our future work list will include transferability tests for the on-site TB parameters as well as the repulsive EAM energies. The parameters of Boron (B-B, B-Mo and B-Si) will be developed in a similar manner. Ultimately, we want our parameters to be applicable in multi-phase, multi-component computations, such as in the Grand Canonical Monte Carlo simulations to predict the phase diagrams.

References

- [1] A.K. McMahan and J.E. Klepeis, Phys. Rev. B **56**, 12250.
- [2] A.K. McMahan and J.E. Klepeis, Mat. Res. Soc. Symp. Proc. **491**, 199.
- [3] J.C. Slater and G.F. Koster, Phys. Rev. **94**, 1498.
- [4] D.A. Papaconstantopoulos, *Handbook of the Band Structure of Elemental Solids*, Plenum, New York, 1986.
- [5] D.A. Papaconstantopoulos and M.J. Mehl, Phys. Rev. B **54**, 4519; S.H. Yang, M.J. Mehl, D.A. Papaconstantopoulos, *ibid.* **57**, R2013.
- [6] D.L. Price and B.R. Cooper, Phys. Rev. B **39**, 4945; D.L. Price, J.M. Wills and B.R. Cooper, *ibid.* **46**, 11368.
- [7] D. Djajaputra and B.R. Cooper, Phys. Stat. Sol. **B236**, 97.
- [8] O.K. Andersen and O. Jepsen, Phys. Rev. Lett. **53**, 2571.
- [9] Th. Frauenheim, F. Weich, Th. Köhler, S. Uhlmann, D. Porezag and G. Seifert, Phys. Rev. B **52**, 11492; J. Widany, Th. Frauenheim, Th. Köhler, M. Sternberg, D. Porezag, G. Jungnickel and G. Seifert, *ibid.* **53**, 4443.
- [10] C.L. Briant, Mat. Res. Soc. Symp. Proc. **322**, 461
- [11] J.H. Schneibel, C.T. Liu, D.S. Easton and C.A. Carmichael, Mat. Sci. Eng. **A261**, 78; I. Rosales and J.H. Schneibel, Intermetallics **8**, 885;

- H. Choe, D. Chen, J.H. Schneibel and R.O. Ritchie, *ibid.* **9**, 209; J.H. Schneibel, C.J. Rawn, T.R. Watkins and E.A. Payzant, *Phys. Rev. B* **65**, 134112.
- [12] C.L. Fu, X. Wang, Y.Y. Ye and K.M. Ho, *Intermetallics* **7**, 179; C.L. Fu and X. Wang, *Phil. Mag. Lett.* **80**, 683.
- [13] R.E. Cohen, M.J. Mehl and D.A. Papaconstantopoulos, *Phys. Rev. B* **50**, 14694.
- [14] C.Z. Wang, B.C. Pan, M.S. Tang, H. Haas, M. Sigalas, G.D. Lee and K.M. Ho, *Mat. Res. Soc. Symp. Proc.* **491**, 211.
- [15] See for example, N.W. Ashcroft and N.D. Mermin, *Solid State Physics* (Saunders Colledge, Philadelphia, 1976), 425.